In Vitro Epiretinal Membrane Model and Antibody Permeability: Relationship With Anti-VEGF Resistance in Diabetic Macular Edema

Rina Namba,[1] Hiroki Kaneko,[1] Ayana Suzumura,[1] Hideyuki Shimizu,[1] Keiko Kataoka,[1] Kei Takayama,[2] Kazuhisa Yamada,[1] Yasuhito Funahashi,[3] Seina Ito,[1] Norie Nonobe,[1] and Hiroko Terasaki[1]

[1]Department of Ophthalmology, Nagoya University Graduate School of Medicine, Nagoya, Japan
[2]Department of Ophthalmology, National Defense Medical College, Tokorozawa, Japan
[3]Department of Urology, Nagoya University Graduate School of Medicine, Nagoya, Japan

PURPOSE. Diabetic macular edema (DME) is characterized by an accumulation of fluid in the macula due to diabetic retinopathy. Currently, anti-VEGF drugs are the standard treatment worldwide for DME. This study aimed to assess whether the existence of epiretinal membrane (ERM) affects anti-VEGF efficacy, due to reduced permeability of the antibody through the ERM.

METHODS. We retrospectively examined clinical data of DME patients who underwent anti-VEGF treatment and evaluated whether clinical differences existed between DME eyes with ERM and those without ERM. We then created an in vitro ERM model using MIO-M1, ARPE-19, and NTI-4 cells on Transwell membranes and evaluated antibody permeability through this in vitro ERM model using fluorescently labeled antibodies.

RESULTS. Central retinal thickness (CRT) change between before and 1 month after first anti-VEGF treatment, as well as final CRT and final visual acuity 12 months after first anti-VEGF treatment, significantly differed between DME eyes with ERM and those without ERM. The in vitro ERM model led to production of collagen I in a manner similar to that of human ERM specimens. Fluorescence intensity of the lower chamber of the in vitro ERM model was significantly reduced in a dose-dependent manner.

CONCLUSIONS. Clinical data analysis indicated that the existence of ERM in DME eyes lowered the efficacy of anti-VEGF treatment. Reduced antibody permeability through the in vitro ERM model suggested ERM presence was associated with resistance to anti-VEGF treatment in DME eyes with ERM.

Keywords: diabetic macular edema, epiretinal membrane, anti-VEGF antibody, Transwell

The number of patients with diabetes is growing rapidly worldwide; it is estimated that 415 million adults had diabetes in 2015, and that the number of patients with diabetes will increase to 622 million by 2040.[1] Because of the increased number of patients with diabetes, the number of patients with diabetic retinopathy (DR) is expected to increase.[2,3] DR is a major vision-threatening disease in adults and constitutes an important microvascular complication caused by diabetes.[3–6] Notably, DR is characterized by extensive vascular leakage, retinal neovascularization, and fibrovascular proliferative growth.[4] Various factors (e.g., hyperglycemia, hypertension, and dyslipidemia) are reportedly involved in DR, and retinal ischemia is strongly related to DR severity.[7–11] Diabetic macular edema (DME) involves accumulation of fluid in the macula due to DR; notably, DME can be diagnosed at any stage of DR. The prevalence of DME is 6.8%; the number of DME patients worldwide was estimated to be 21 million in 2010.[3] VEGF plays a pivotal role in the pathogenesis of DME, such that anti-VEGF drugs are currently the standard treatment worldwide for DME.[12–15]

The prevalence of vitreomacular interface abnormalities (VMIA), including epiretinal membrane (ERM), is reportedly higher in patients with DME.[16–19] VMIA includes ERM, as well as vitreomacular adhesion (VMA), vitreomacular traction (VMT), and incomplete posterior vitreous detachment (PVD); these abnormalities are associated with pathological changes in the interface between the vitreous and sensory retina.[20–22] Consistent with the concept that VMIA is a pathogenic aspect of DME, previous studies showed benefits associated with removal of VMIA for treatment of DME.[23–25] Other studies suggested that DME patients with ERM showed worse final visual acuity[18,26,27] and greater central retinal thickness (CRT).[18] However, a clear underlying mechanism has not been elucidated regarding this resistance to anti-VEGF treatment among DME patients with ERM. We hypothesized that the existence of ERM reduces anti-VEGF drug permeability (i.e., directly through the ERM) in the retina. To test our hypothesis, we retrospectively examined clinical data of DME patients undergoing treatment with ranibizumab (Lucentis; Novartis Pharma AG, Basel, Switzerland, and Genentech Inc., South San Francisco, CA, USA) to evaluate whether clinical differences

exist between DME eyes with ERM and those without ERM. Additionally, we constructed an in vitro ERM model using cell lines representative of human ERM specimens, and evaluated antibody permeability in the context of the existence of in vitro ERM.

METHODS

We retrospectively studied DME patients, and divided these patients into two groups as follows: "DME with ERM" and "DME without ERM". The diagnosis of ERM was based on clinical, funduscopic examination by a retinal specialist (HK), as well as ocular imaging analysis. Related medical records were carefully reviewed, including duration of subjective metamorphopsia, simultaneous cataract, duration of symptoms, ophthalmologic treatments, and the presence of other retinal alterations.[28] The inclusion criteria for patients were as follows: (1) diagnosis of DME (CRT $\geq$ 250 µm)[29,30] that required treatment with ranibizumab; (2) absence of unexpected complications during anti-VEGF treatment for 12 months; (3) successful performance of optical coherence tomography (OCT) imaging (Cirrus OCT; Carl Zeiss Meditec, Dublin, CA, USA) during the study (signal strength $\geq$ 7). The exclusion criteria were as follows: (1) eyes with a history of vitrectomy for other diseases or corneal surgeries; (2) eyes in patients who had any ocular or systemic disorder that could affect retinal thickness (e.g., glaucoma, optic nerve diseases, or AMD); (3) eyes with VMT; (4) eyes that received other anti-VEGF drugs (i.e., not ranibizumab). The Nagoya University Hospital Ethics Review Board approved this retrospective analysis of patients' data and waived the requirement for informed consent. We measured average retinal thicknesses using the Early Treatment Diabetic Retinopathy Study (ETDRS) chart[31,32] before and 1 and 12 months after the initiation of anti-VEGF treatment.

Sample Collection From Patients With DME and Immunostaining

Each ERM specimen was collected during vitrectomy surgery for ERM. The tissue was immediately fixed with 4% paraformaldehyde and cryoprotected; then, 10-µm sections were obtained, as previously described.[33,34] The sections were stained with hematoxylin and eosin, or immunostained with anti-alpha smooth muscle actin (αSMA) antibody (1:200; Sigma-Aldrich, St. Louis, MO, USA), anti-glial fibrillary acidic protein (GFAP) antibody (1:400; Cell Signaling Technology, Danvers, MA, USA), and anti-collagen type I antibody (1:200; Rockland Immunochemicals, Inc., Limerick, PA, USA); they were then visualized with Alexa 488- and Alexa 594-conjugated antibodies (1:1000; Invitrogen, Carlsbad, CA, USA), as well as 4', 6-diamidino-2-phenylindole (DAPI; Invitrogen). Images were acquired with a BioImaging Navigator fluorescence microscope (BZ-9000; Keyence, Osaka, Japan). This study was conducted in accordance with the guidelines of the Declaration of Helsinki; the protocol was registered within the UMIN Clinical Trial Registry (registered number UMIN000024553) and approved by the Nagoya University Hospital Ethics Review Board. Written informed consent was obtained from all participating patients.

In Vitro ERM Model and Antibody Permeabilization Assay

Based on a previous study involving cultured RPE cells,[35–39] we used a modified Transwell system (#353504 & #353495; Corning, Corning, NY, USA) in this study. The number of cells that were seeded on the membrane was determined on the basis of previous studies.[35,39] Cultured MIO-M1 cells were purchased from E-lucid (University College London, London, UK), cultured ARPE-19 cells were purchased from the American Type Culture Collection (Rockville, MD, USA), and NTI-4 cells were purchased from the Japanese Collection of Research Bioresource Cell Bank (Ibaraki, Osaka, Japan). The cells were grown in Dulbecco's modified Eagle's medium (Sigma-Aldrich) and supplemented with 10% fetal bovine serum (Gibco, Waltham, MA, USA) and 1% penicillin–streptomycin (Merck KGaA, Darmstadt, Germany). MIO-M1 alone or a combination of MIO-M1, ARPE-19, and NTI-4 cells (each 4.7×10^4, or 14.1×10^4 in total) were seeded onto Transwell filters precoated with extracellular matrix (ECM, BD Biosciences, San Jose, CA, USA). Cells were cultured for 7 days prior to antibody permeabilization assays. To equalize the surface levels of medium in the upper and lower chambers, 300 µL of medium was placed in the upper chamber and 900 µL of medium was placed in the lower chamber. Ranibizumab was labeled with FITC using a conjugation kit (Fluoro Tag; Sigma-Aldrich), in accordance with the manufacturer's protocol. Naked FITC, FITC-labeled ranibizumab, or IgG F(ab')2 tagged with Alexa Fluor 488 (Alexa 488 Fab; 1:500; #A11070; Invitrogen) were added to the upper chamber. After incubation (1, 6, 24, 48, and 72 hours), the medium was removed from the upper and lower chambers (80-µL each), and fluorescence intensity was measured in each sample (PowerScan4 plate reader; DS Pharma Biomedical, Osaka, Japan).

Statistics

For DME patients, we expressed data as medians. In cases where one patient received treatment for both right and left eyes, we counted each eye individually ($n = 2$). We compared parameters between DME patients with and without ERM using the Mann-Whitney U test. For in vitro assays, we expressed data as means $\pm$ standard deviations (n = number of samples). F test and Student's t-test or Welch's t-test were used to compare results. P values < 0.05 were considered to be statistically significant in all analyses.

RESULTS

DME Patients' Characteristics and Their Association With ERM

Of more than 500 first-visit DME patients in our hospital during the period from February 2014 to August 2018, only 43 eyes of 35 patients with DME were included in this study. The majority of DME patients were excluded because their anti-VEGF treatment had been changed within the study period. The demographic and clinical characteristics of the included patients are listed in Table 1. The median patient age was 61.0 years; there were 16 DME patients with ERM and 19 DME patients without ERM. Representative images of the color fundus outlined by ETDRS sectors and ETDRS-based retinal thickness, as well as horizontal OCT images before and 12 months after the initiation of anti-VEGF treatment, are shown in Figure 1. Regional retinal thicknesses, based on central sectors from ETDRS before and 1 and 12 months after the initiation of anti-VEGF treatment, as well as visual acuity and the number of intravitreal injections of anti-VEGF drug, are listed in Table 2. Changes in CRT before and 1 month after the initiation of anti-VEGF treatment, as well as final CRT and final visual acuity 12 months after the initiation of anti-VEGF treatment, significantly differed between DME eyes with ERM and those without ERM.

TABLE 1. Demographic and Clinical Characteristics of DME Patients

	DME	DME+ERM	P Value
Number of eyes	25	18	
Age (y)	66.0 (59.0–71.0)	67.5 (62.5–71.8)	0.482
Sex (M/F)	17/8	13/5	0.766
Duration of diabetes (y)	10.0 (8.0–20.0)	14.0 (10.0–25.0)	0.249
HbA1c (%)	6.8 (6.3–7.8)	7.1 (6.6–7.4)	0.576
Type of diabetes (type 1/type 2)	0/25	0/18	
Stage of DR			
No DR (%)	0 (0)	0 (0)	
Mild NPDR (%)	0 (0)	0 (0)	
Moderate NPDR (%)	4 (16)	2 (11)	0.648
Severe NPDR	16 (64)	12 (67)	0.856
PDR (%)	5 (20)	4 (22)	0.860
Previous laser surgery			
None (%)	7 (28)	3 (17)	0.386
Macular laser (%)	0 (0)	0 (0)	
PRP (%)	18 (72)	14 (78)	0.668
Macular laser+PRP (%)	0 (0)	1 (5)	
Previous cataract surgery (%)	5 (20)	5 (28)	0.552
History of hypertension (%)	9 (36)	10 (56)	0.203
History of kidney disease (%)	4 (16)	6 (34)	0.184
Posterior hyaloid detached at baseline (%)	17 (68)	12 (67)	0.927

NPDR, nonproliferative DR; PDR, proliferative DR; PRP, panretinal photocoagulation.

Cell Types in ERM Specimen in DME Eye

We obtained ERM tissue from a 63-year-old female DME patient with ERM. Phase-contrast microscopy showed pigmented cells in the tissue, indicating that the ERM specimen included migrated RPE cells. Immunohistochemical analysis also showed GFAP- and αSMA-positive cells. These images indicated that the ERM specimen included cells that had originated from RPE, Müller, and fibroblast cells (Fig. 2).

In Vitro ERM Model

Based on our immunohistochemical analysis and previous studies,[40–44] we designed an in vitro ERM model (Fig. 3). ECM placed on the Transwell membrane served as internal limiting membrane (ILM); the cell complex (MIO-M1, ARPE-19, and NTI-4 cells) served as ERM. We first measured time-dependent change in Alexa 488 Fab-based fluorescence intensity in the lower chamber through ECM alone (no ERM). The fluorescence intensity of Alexa 488 Fab in the lower chamber through ECM alone increased in a time-dependent manner until the 48-hour time point, then decreased between the 48- and 72-hour time points (Fig. 4A). In addition, the fluorescence intensities in the lower chamber did not significantly differ between ECM(−) and ECM(+) cultures (86.67 vs. 80.83, $n = 6$, $P = 0.42$, Fig. 4B). These data indicated that the presence of ECM did not affect Fab permeability. Seeding MIO-M1, ARPE-19, and NTI-4 cells on the Transwell membrane led to production of collagen I (Fig. 4D) in a manner similar to that of human ERM specimens (Fig. 4C). In addition, MIO-M1, ARPE-19, and NTI-4 cells on the
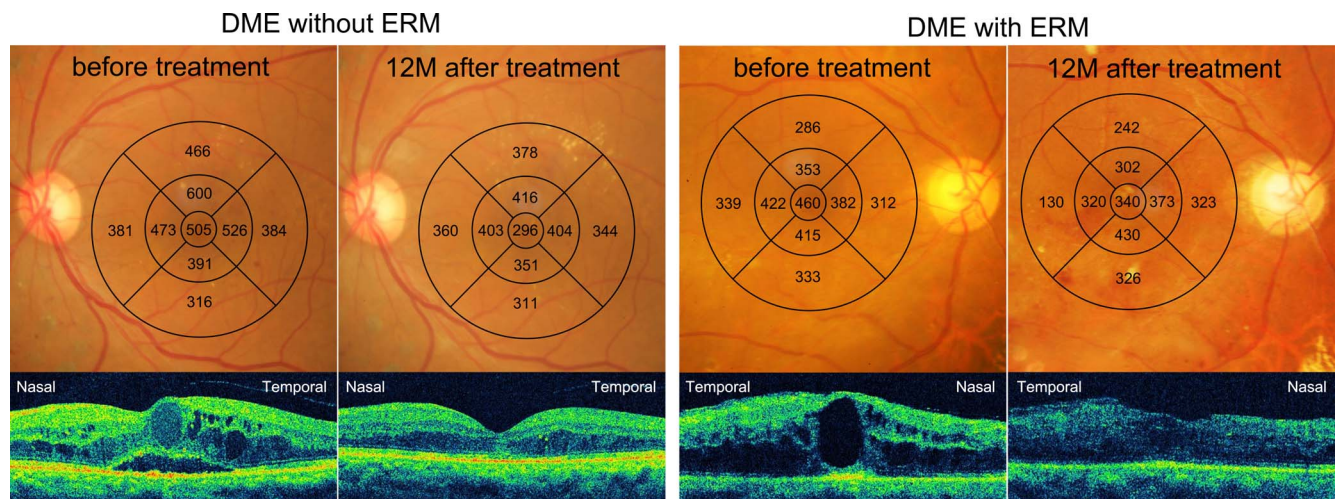

FIGURE 1. Representative images in DME eyes with or without ERM. Representative color fundus images and horizontal foveal images captured by OCT, as well as mean regional retinal thickness dependent on ETDRS sectors, before and 12 months (12M) after the initiation of anti-VEGF treatment. The DME eye without ERM shows a robust response to anti-VEGF treatment with reduced central retinal thickness, whereas the DME eye with ERM shows moderate recovery after anti-VEGF treatment with moderately sustained DME (340 μm), 12M after anti-VEGF treatment.
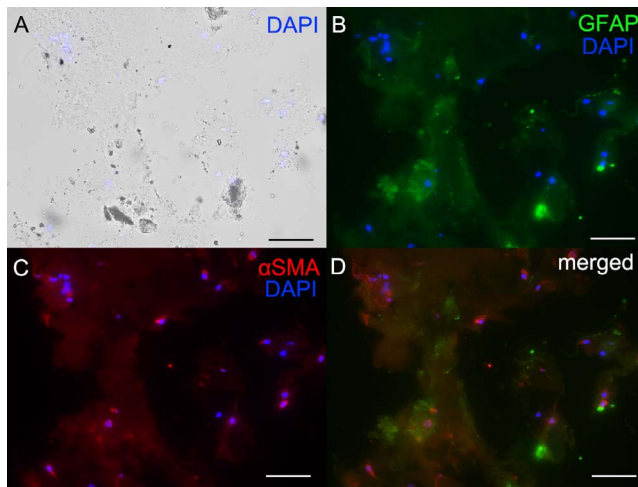
FIGURE 2. Immunohistochemistry results of ERM tissue from DME eyes. The images show a phase-contrast micrograph merged with DAPI (**A**), anti-GFAP staining merged with DAPI (**B**), anti-αSMA staining merged with DAPI (**C**), and anti-GFAP and anti-αSMA staining merged with DAPI (**D**). The phase-contrast micrograph shows pigmented cells in ERM specimens, indicating that the ERM contains RPE cells. The presence of GFAP- and αSMA-positive cells indicates that the ERM comprises Müller cells and fibroblast cells. *Scale bars*: 50 μm.

FIGURE 3. Schematic drawing of in vitro ERM model. After plating human ECM on the Transwell membrane, MIO-M1 cells alone or MIO-M1/ARPE-19/NTI-4 combination were cultured for 7 days. Alexa 488 Fab, naked FITC, or FITC-labeled ranibizumab were added to the medium in the upper chamber and the fluorescence intensity of the medium was measured. ECM(−) indicates Transwell only. ECM(+) indicates ECM placed on the Transwell. ECM(+)ERM(+) indicates MIO-M1 cells alone or MIO-M1/ARPE-19/NTI-4 cultured on ECM and Transwell; this was used as an in vitro ERM model.

Transwell membrane formed a multilayer configuration (Fig. 4F) in a manner similar to that of human ERM specimens (Fig. 4E). The fluorescence intensities of naked FITC did not significantly differ between ECM(+) and ERM(+) in the upper chamber (91.47 vs. 94.07, $n = 5$, $P = 0.63$) or lower chamber (54.17 vs. 53.75, $n = 12$, $P = 0.88$, Fig. 4G).

Association Between ERM and Antibody Permeabilization In Vitro

We next measured Alexa 488 Fab fluorescence intensity in the lower chamber of the in vitro ERM model using MIO-M1 alone or the combination of MIO-MI, ARPE-19, and NTI-4 cells (Figs. 5A, 5B). Compared with the ECM group (no cells, 101.33), the fluorescence intensities of the Alexa 488 Fab in the lower chamber of the MIO-M1 alone group (61.72, $P = 4.45 \times 10^{-3}$) and MIO-M1/ARPE-19/NTI-4 combined group (54.00, $P = 2.18 \times 10^{-7}$) were significantly reduced (Fig. 5A). In addition, compared with the ECM group (no cells, 119.00), the fluorescence intensity of Alexa 488 Fab in the upper chamber of the MIO-M1 alone group (189.83) was significantly higher ($P = 3.08 \times 10^{-3}$), and that of the MIO-M1/ARPE-19/NTI-4
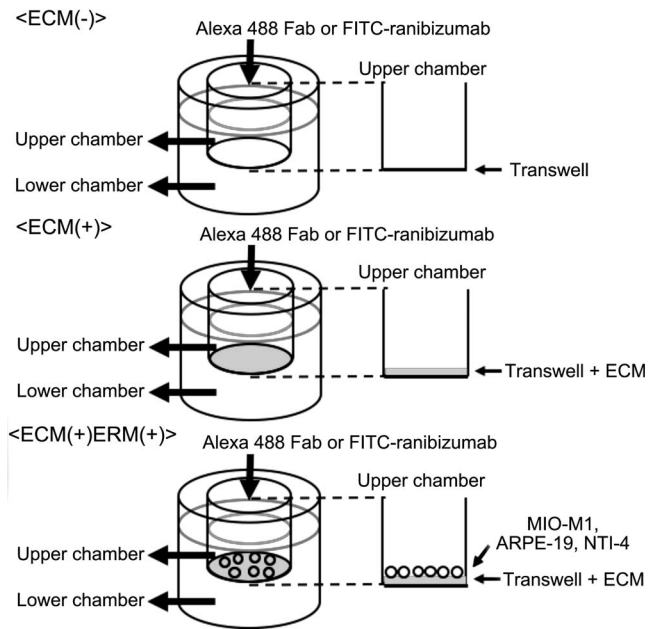
combined group (172.17) tended to be higher ($P = 1.31 \times 10^{-2}$, Fig. 5A). Furthermore, compared with the ECM group (no cells, 101.33), the fluorescence intensities of Alexa 488 Fab in the lower chamber in the MIO-M1/ARPE-19/NTI-4 combined group with 4.7×10^4 cells (67.50, $P = 1.33 \times 10^{-6}$) and in the group with 14.1×10^4 cells (54.00, $P = 2.18 \times 10^{-7}$) were significantly reduced in a dose-dependent manner (Fig. 5B). In addition, compared with the ECM group (no cells, 119.00), the fluorescence intensities of Alexa 488 Fab in the upper chamber of the MIO-M1/ARPE-19/NTI-4 combined group with 4.7×10^4 cells (157.67, $P = 4.23 \times 10^{-2}$) and in the group with 14.1×10^4 cells (172.17, $P = 1.31 \times 10^{-2}$) were significantly increased in a dose-dependent manner (Fig. 5B). Similarly, we measured FITC-labeled ranibizumab fluorescence intensity in the upper and lower chambers of the in vitro ERM model using MIO-M1 alone or the combination of MIO-MI, ARPE-19, and NTI-4 cells

TABLE 2. Central Retinal Thickness, Visual Acuity, and Number of Intravitreal Injections of Anti-VEGF in DME Patients

|	DME ($n = 25$)	DME+ERM ($n = 18$)	P Value
CRT			
baseline	475.00 (419.00–580.00)	440.00 (375.25–521.25)	0.23
1 mo after treatment	330.00 (287.00–360.00)	385.00 (299.50–454.00)	0.18
12 mo after treatment	311.00 (281.00–347.00)	382.00 (334.25–520.25)	0.01
CRT change			
1 mo/baseline	74.22 (57.63–84.81)	88.12 (70.52–94.35)	0.02
Visual acuity			
baseline	0.30 (0.22–0.52)	0.40 (0.30–0.68)	0.47
12 mo after treatment	0.22 (0.05–0.30)	0.40 (0.22–0.77)	0.04
Number of injections			
During 12 mo after treatment	4.00 (2.00–5.00)	2.00 (1.25–4.75)	0.30

Median (Q1–Q3).
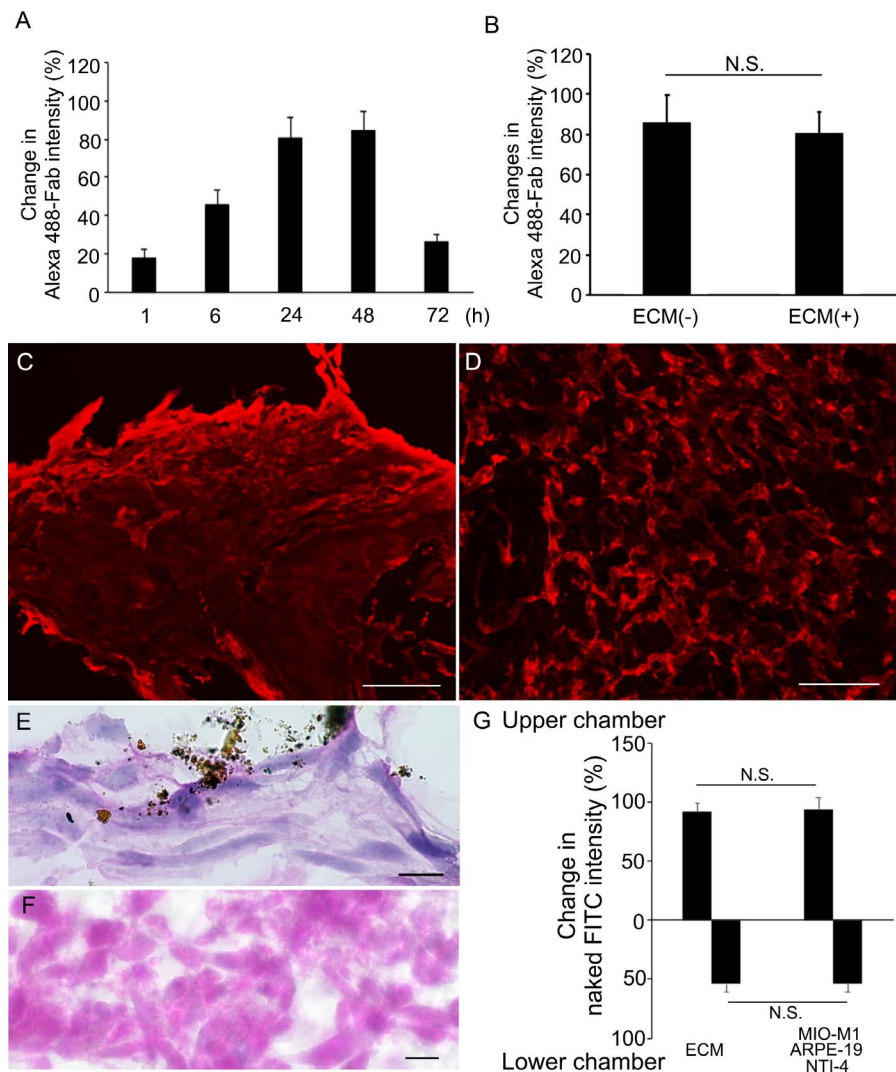
FIGURE 4. Fluorescence intensity through Transwell and ECM. Human ECM was placed on the Transwell membrane, to serve as internal limiting membrane. (**A**) Alexa 488 Fab was added in the upper chamber and fluorescence intensity was measured in the lower chamber. Fluorescence intensity increased in a time-dependent manner until the 48-hour time point in the lower chamber, through ECM alone. (**B**) Fluorescence intensities in the lower chamber of the ECM(−) and ECM(+) conditions at 24 hours were not significantly different (86.67 vs. 80.83, $n = 6$, $P = 0.42$). (**C**, **D**) Collagen I staining of surgically excised ERM specimen (**C**) and in vitro ERM model (**D**). (**E**, **F**) Hematoxylin and eosin staining showed multilayered structure of surgically excised ERM specimen (**E**) and in vitro ERM model (**F**). (**G**) Naked FITC was added in the medium of the upper chamber; the fluorescence intensity of FITC was measured in the medium of upper and lower chambers through ECM alone (no cells) and MIO-M1/ARPE-19/NTI-4 combination (each cell type 4.7×10^4 cells/well). Fluorescence intensities of FITC in upper and lower chambers were not significantly different. *Scale bars*: 10 μm in (**E**, **F**) and 100 μm in (**C**, **D**).

(Fig. 5C) to exclude the possibility that goat IgG F(ab')2 and ranibizumab react differently to in vitro ERM model that is composed of human cells. Compared with the ECM group (no cells, 68.79) the FITC intensities of FITC-labeled ranibizumab in the lower chamber of the MIO-M1/ARPE-19/NTI-4 combined group with 4.7×10^4 cells (54.17, $P = 4.12 \times 10^{-5}$) and in the group with 14.1×10^4 cells (38.67, $P = 9.19 \times 10^{-8}$) were significantly decreased in a dose-dependent manner (Fig. 5C). In addition, compared with the ECM group (no cells, 200.79), the fluorescence intensities of FITC-labeled ranibizumab in the upper chamber of the MIO-M1/ARPE-19/NTI-4 combined group with 4.7×10^4 cells (221.79, $P = 2.92 \times 10^{-2}$) and in the group with 14.1×10^4 cells (237.79, $P = 1.59 \times 10^{-3}$) were significantly increased in a dose-dependent manner (Fig. 5C). These results indicated that the existence of ERM component cells (MIO-M1/ARPE-19/NTI-4) reduced antibody permeabilization in the in vitro ERM model.

DISCUSSION

In this study, change in CRT after first ranibizumab injection, final CRT, and final visual acuity strongly suggested that DME eyes with ERM exhibited worse responses after anti-VEGF treatment, compared with those without ERM. Previous studies have revealed conflicting results regarding the influence of VMIA on anti-VEGF treatment in DME. The Diabetic Retinopathy Clinical Research Network reported that treatment with ranibizumab is effective in cases of DME involving younger patients, lower grade of retinopathy, and eyes without retina wrinkle.[27] In our study, there were no significant differences in age or grade of retinopathy; therefore, these factors presumably did not affect differences in CRT and final visual acuity. Yoon et al.[26] reported that DME eyes with VMIA had smaller visual improvement after three injections of anti-VEGF drugs. Wong et al.[18] reported that the presence of ERM
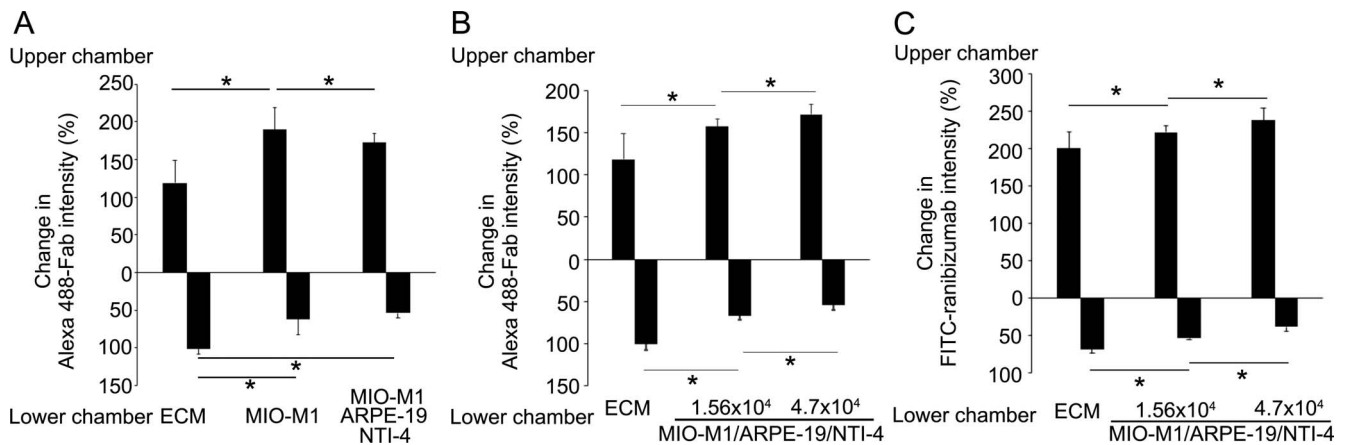
FIGURE 5. Difference in fluorescence intensity through in vitro ERM model. (**A**) Alexa 488 Fab was added in the medium of the upper chamber and fluorescence intensity was measured in the medium of upper and lower chambers through ECM alone (no cells), MIO-MI cells alone (4.7×10^4 MIO-M1 cells/well), and MIO-M1/ARPE-19/NTI-4 combination (each cell type, 1.56×10^4 cells/well). Fluorescence intensity of Alexa 488 Fab in the lower chamber was reduced through MIO-M1 and MIO-M1/ARPE-19/NTI-4 ($n = 6$). (**B**) Alexa 488 Fab was added in the medium of the upper chamber and fluorescence intensity was measured in the medium of upper and lower chambers through ECM alone (no cells) and MIO-M1/ARPE-19/NTI-4 combination (each cell type, 1.56×10^4 cells/well and 4.7×10^4 cells/well, respectively). Fluorescence intensity of Alexa 488 Fab in the lower chamber was reduced through MIO-M1/ARPE-19/NTI-4 in a cell number-dependent manner ($n = 6$). (**C**) FITC-conjugated ranibizumab was added in the medium of the upper chamber and fluorescence intensity of FITC was measured in the medium of upper and lower chambers through ECM alone (no cells) and MIO-M1/ARPE-19/NTI-4 (each cell type, 1.56×10^4 cells/well and 4.7×10^4 cells/well, respectively). Fluorescence intensity of FITC in the lower chamber was reduced through MIO-M1/ARPE-19/NTI-4 in a cell number-dependent manner ($n = 8$). *Upward* and *downward bars* in the graph indicate fluorescence intensity in upper and lower chambers, respectively.

restricted functional (vision) and anatomic (CRT) improvements in DME. The prior findings are thus consistent with those of our study. Conversely, a retrospective cohort study showed that eyes with evidence of VMA (except for VMT) at baseline exhibited better visual acuity improvement, compared with those without VMA, at 6 months after treatment with ranibizumab.[45] However, in that previous study, seven of 26 patients with VMA exhibited PVD within the evaluation period. Although there was no statistically significant difference relative to the findings in the 17 patients who did not show changes in VMA, the eye with PVD was reported to exhibit better BCVA improvement and CRT reduction.[45] In our current study, changes in PVD were not recognized within the study period, and the ERM did not show robust changes.

In addition to analyzing clinical data, we also examined the association between ERM and anti-VEGF drugs through biological experiments using cultured cells. Immunostaining of ERM from DME eyes with ERM showed GFAP-positive, αSMA-positive, and pigmented cells, suggesting that Müller, fibroblast, and RPE cells were present; this was consistent with the findings of previous reports.[40,43,44,46] Idiopathic ERM is reportedly formed by the growth of glial cells,[42] suggesting that it may be derived from Müller glia cells.[43] Moreover, ERM has been reported to contain myofibroblasts,[40,43,44,46] and RPE cells have been observed in ERM after retinal breaks.[40,41] Therefore, we chose to use three different types of cells as membrane that simulates ERM as follows: ARPE-19 cells (RPE), MIO-M1 cells (Müller glia), and NTI-4 cells (myofibroblasts).

The in vitro ERM model in this study, described in the prior paragraph, significantly reduced fluorescence intensity in the lower chamber; in contrast, it enhanced fluorescence intensity (remnant) in the upper chamber as the number of cells increased. In addition, when the total number of cells was similar, the antibodies showed a reduced tendency to permeate through the in vitro ERM model comprising a mixture of MIO-M1, NTI-4, and ARPE-19 cells, compared with the in vitro ERM model comprising MIO-M1 cells alone; notably, this difference was not significant. Because the size of the Alexa 488 Fab used is smaller than the pore size of the Transwell filter, the

Transwell filter did not directly interfere with antibody permeabilization. In addition, the fluorescence level of Alexa 488 Fab was unlikely to be attenuated at 24 hours (Fig. 4A) and ECM was unlikely to directly interfere with antibody permeabilization (Fig. 4B). Therefore, in our in vitro ERM model, the reduced antibody permeabilization was caused by the ERM itself. Additionally, our in vitro ERM model produced collagen type I in a manner similar to that of human ERM samples, and may be useful as a novel in vitro model to study ERM.

The limitations of this study were as follows: (1) the Alexa 488 Fab comprised an antibody derived from an animal. Therefore, we cannot exclude the possibility that nonhuman IgG had unexpected biological reaction with human cells. (2) The ERM diagnostic criteria were not strictly controlled. A previous report noted that ERM was recognized by OCT as thin, hyperreflective bands anterior to the retina, or bright red bands in a pseudocolored image.[47] The diagnosis of globally adherent ERM by spectral-domain OCT is based on a difference in brightness (or in bright red color on pseudocolored image) of the surface tissue; this is more evident in spectral domain OCT than in conventional OCT.[48] However, there are various types of ERM, and we did not strictly define or categorize ERM in this study. (3) Although the results from previous clinical studies indicated that the effect of ERM on the anti-VEGF treatment is due to the adhesion of ERM as well as its traction, our in vitro ERM model is suitable as a VMA model, but not as a VMT model. Accordingly, in our clinical study, we excluded patients with VMT; therefore, our current study solely evaluated the effect of ERM and its adhesion on anti-VEGF treatment, rather than the effect of traction. (4) The ratio of RPE, Müller, and fibroblast cells might vary among ERM specimens; thus, our in vitro ERM model does not completely reflect the pathology of reduced antibody permeabilization through the ERM.

In conclusion, based on the results of our clinical and biological analysis, we suspect that the resistance of DME to anti-VEGF treatment is partially due to increased resistance to antibody permeabilization through the ERM.

Acknowledgments

References

1. Ogurtsova K, da Rocha Fernandes JD, Huang Y, et al. IDF Diabetes Atlas: global estimates for the prevalence of diabetes for 2015 and 2040. *Diabetes Res Clin Pract*. 2017;128:40–50.

2. Lövestam-Adrian M, Agardh CD, Torffvit O, Agardh E. Diabetic retinopathy, visual acuity, and medical risk indicators: a continuous 10-year follow-up study in Type 1 diabetic patients under routine care. *J Diabetes Complications*. 2001;15:287–294.

3. Yau JW, Rogers SL, Kawasaki R, et al. Global prevalence and major risk factors of diabetic retinopathy. *Diabetes Care*. 2012;35:556–564.

4. Antonetti DA, Klein R, Gardner TW. Diabetic retinopathy. *N Engl J Med*. 2012;366:1227–1239.

5. Congdon NG, Friedman DS, Lietman T. Important causes of visual impairment in the world today. *JAMA*. 2003;290:2057–2060.

6. Fong DS, Aiello LP, Ferris FL, Klein R. Diabetic retinopathy. *Diabetes Care*. 2004;27:2540–2553.

7. Nathan DM, Genuth S, Lachin J, et al. The effect of intensive treatment of diabetes on the development and progression of long-term complications in insulin-dependent diabetes mellitus. *N Engl J Med*. 1993;329:977–986.

8. Rema M, Srivastava BK, Anitha B, Deepa R, Mohan V. Association of serum lipids with diabetic retinopathy in urban South Indians–the Chennai Urban Rural Epidemiology Study (CURES) Eye Study–2. *Diabet Med*. 2006;23:1029–1036.

9. Wong TY, Cheung N, Tay WT, et al. Prevalence and risk factors for diabetic retinopathy: the Singapore Malay Eye Study. *Ophthalmology*. 2008;115:1869–1875.

10. Klein R, Knudtson MD, Lee KE, Gangnon R, Klein BE. The Wisconsin Epidemiologic Study of Diabetic Retinopathy: XXII the twenty-five-year progression of retinopathy in persons with type 1 diabetes. *Ophthalmology*. 2008;115:1859–1868.

11. Nagaoka T, Sato E, Takahashi A, Yokota H, Sogawa K, Yoshida A. Impaired retinal circulation in patients with type 2 diabetes mellitus: retinal laser Doppler velocimetry study. *Invest Ophthalmol Vis Sci*. 2010;51:6729–6734.

12. Stewart MW. Anti-VEGF therapy for diabetic macular edema. *Curr Diab Rep*. 2014;14:510.

13. Mitchell P, Bandello F, Schmidt-Erfurth U, et al. The RESTORE study: ranibizumab monotherapy or combined with laser versus laser monotherapy for diabetic macular edema. *Ophthalmology*. 2011;118:615–625.

14. Ishibashi T, Li X, Koh A, et al. The REVEAL Study: ranibizumab monotherapy or combined with laser versus laser monotherapy in Asian patients with diabetic macular edema. *Ophthalmology*. 2015;122:1402–1415.

15. Nguyen QD, Brown DM, Marcus DM, et al. Ranibizumab for diabetic macular edema: results from 2 phase III randomized trials: RISE and RIDE. *Ophthalmology*. 2012;119:789–801.

16. Ghazi NG, Ciralsky JB, Shah SM, Campochiaro PA, Haller JA. Optical coherence tomography findings in persistent diabetic macular edema: the vitreomacular interface. *Am J Ophthalmol*. 2007;144:747–754.

17. Kim BY, Smith SD, Kaiser PK. Optical coherence tomographic patterns of diabetic macular edema. *Am J Ophthalmol*. 2006; 142:405–412.

18. Wong Y, Steel DHW, Habib MS, et al. Vitreoretinal interface abnormalities in patients treatedwith ranibizumab for diabetic macular oedema. *Graefes Arch Clin Exp Ophthalmol*. 2017; 255:733–742.

19. Akbar Khan I, Mohamed MD, Mann SS, Hysi PG, Laidlaw DA. Prevalence of vitreomacular interface abnormalities on spectral domain optical coherence tomography of patients undergoing macular photocoagulation for centre involving diabetic macular oedema. *Br J Ophthalmol*. 2015;99:1078–1081.

20. Tamura K, Yokoyama T, Ebihara N, Murakami A. Histopathologic analysis of the internal limiting membrane surgically peeled from eyes with diffuse diabetic macular edema. *Jpn J Ophthalmol*. 2012;56:280–287.

21. Gandorfer A, Rohleder M, Grosselfinger S, Haritoglou C, Ulbig M, Kampik A. Epiretinal pathology of diffuse diabetic macular edema associated with vitreomacular traction. *Am J Ophthalmol*. 2005;139:638–652.

22. Duker JS, Kaiser PK, Binder S, et al. The International Vitreomacular Traction Study Group classification of vitreomacular adhesion, traction, and macular hole. *Ophthalmology*. 2013;120:2611–2619.

23. Lewis H, Abrams GW, Blumenkranz MS, Campo RV. Vitrectomy for diabetic macular traction and edema associated with posterior hyaloidal traction. *Ophthalmology*. 1992;99:753–759.

24. Shah SP, Patel M, Thomas D, Aldington S, Laidlaw DA. Factors predicting outcome of vitrectomy for diabetic macular oedema: results of a prospective study. *Br J Ophthalmol*. 2006;90:33–36.

25. Haller JA, Qin H, Apte RS, et al. Vitrectomy outcomes in eyes with diabetic macular edema and vitreomacular traction. *Ophthalmology*. 2010;117:1087–1093.

26. Yoon D, Rusu I, Barbazetto I. Reduced effect of anti-vascular endothelial growth factor agents on diabetics with vitreomacular interface abnormalities. *Int Ophthalmol*. 2014;34:817–823.

27. Bressler SB, Qin H, Beck RW, et al. Factors associated with changes in visual acuity and central subfield thickness at 1 year after treatment for diabetic macular edema with ranibizumab. *Arch Ophthalmol*. 2012;130:1153–1161.

28. Pinilla I, Garcia-Martin E, Fernandez-Larripa S, Fuentes-Broto L, Sanchez-Cano AI, Abecia E. Reproducibility and repeatability of Cirrus and Spectralis Fourier-domain optical coherence tomography of healthy and epiretinal membrane eyes. *Retina*. 2013;33:1448–1455.

29. Do DV, Sepah YJ, Boyer D, et al. Month-6 primary outcomes of the READ-3 study (Ranibizumab for Edema of the mAcula in Diabetes-Protocol 3 with high dose). *Eye (Lond)*. 2015;29: 1538–1544.

30. Virgili G, Menchini F, Casazza G, et al. Optical coherence tomography (OCT) for detection of macular oedema in patients with diabetic retinopathy. *Cochrane Database Syst Rev*. 2015;1:CD008081.

31. Early Treatment Diabetic Retinopathy Study Group. Grading diabetic retinopathy from stereoscopic color fundus photographs–an extension of the modified Airlie House classifica-

tion. ETDRS report number 10. *Ophthalmology*. 1991;98: 786–806.

32. Kaneko H, Matsuura T, Takayama K, et al. Increased retinal thinning after combination of internal limiting membrane peeling and silicone oil endotamponade in proliferative diabetic retinopathy. *Ophthalmologica*. 2017;238:226–235.

33. Kaneko H, Ye F, Ijima R, et al. Histamine H4 receptor as a new therapeutic target for choroidal neovascularization in age-related macular degeneration. *Br J Pharmacol*. 2014;171: 3754–3763.

34. Nagasaka Y, Kaneko H, Ye F, et al. Role of caveolin-1 for blocking the epithelial-mesenchymal transition in proliferative vitreoretinopathy. *Invest Ophthalmol Vis Sci*. 2017;58: 221–229.

35. Ye F, Kaneko H, Hayashi Y, et al. Malondialdehyde induces autophagy dysfunction and VEGF secretion in the retinal pigment epithelium in age-related macular degeneration. *Free Radic Biol Med*. 2016;94:121–134.

36. Dunn KC, Aotaki-Keen AE, Putkey FR, Hjelmeland LM. ARPE-19, a human retinal pigment epithelial cell line with differentiated properties. *Exp Eye Res*. 1996;62:155–169.

37. Maminishkis A, Chen S, Jalickee S, et al. Confluent monolayers of cultured human fetal retinal pigment epithelium exhibit morphology and physiology of native tissue. *Invest Ophthalmol Vis Sci*. 2006;47:3612–3624.

38. Sonoda S, Spee C, Barron E, Ryan SJ, Kannan R, Hinton DR. A protocol for the culture and differentiation of highly polarized human retinal pigment epithelial cells. *Nat Protoc*. 2009;4: 662–673.

39. Yoshihara N, Terasaki H, Shirasawa M, et al. Permeability and anti-vascular endothelial growth factor effects of bevacizumab, ranibizumab, and aflibercept in polarized retinal pigment epithelial layer in vitro. *Retina*. 2017;37:179–190.

40. Morino I, Hiscott P, McKechnie N, Grierson I. Variation in epiretinal membrane components with clinical duration of the proliferative tissue. *Br J Ophthalmol*. 1990;74:393–399.

41. Kampik A, Kenyon KR, Michels RG, Green WR, de la Cruz ZC. Epiretinal and vitreous membranes. Comparative study of 56 cases. *Arch Ophthalmol*. 1981;99:1445–1454.

42. Roth AM, Foos RY. Surface wrinkling retinopathy in eyes enucleated at autopsy. *Trans Am Acad Ophthalmol Otolaryngol*. 1971;75:1047–1058.

43. Zhao F, Gandorfer A, Haritoglou C, et al. Epiretinal cell proliferation in macular pucker and vitreomacular traction syndrome: analysis of flat-mounted internal limiting membrane specimens. *Retina*. 2013;33:77–88.

44. Wertheimer C, Eibl-Lindner KH, Compera D, et al. A cell culture technique for human epiretinal membranes to describe cell behavior and membrane contraction in vitro. *Graefes Arch Clin Exp Ophthalmol*. 2017;255:2147–2155.

45. Sadiq MA, Soliman MK, Sarwar S, et al. Effect of vitreomacular adhesion on treatment outcomes in the Ranibizumab for Edema of the Macula in Diabetes (READ-3) Study. *Ophthalmology*. 2016;123:324–329.

46. Vogt D, Vielmuth F, Wertheimer C, et al. Premacular membranes in tissue culture. *Graefes Arch Clin Exp Ophthalmol*. 2018;256:1589–1597.

47. Wilkins JR, Puliafito CA, Hee MR, et al. Characterization of epiretinal membranes using optical coherence tomography. *Ophthalmology*. 1996;103:2142–2151.

48. Koizumi H, Spaide RF, Fisher YL, Freund KB, Klancnik JM, Yannuzzi LA. Three-dimensional evaluation of vitreomacular traction and epiretinal membrane using spectral-domain optical coherence tomography. *Am J Ophthalmol*. 2008; 145:509–517.

Investigative Ophthalmology & Visual Science